Available online at www.sciencedirect.com

SCIENCE DIRECT®

Thermochimica Acta 445 (2006) 86–91

thermochimica acta

www.elsevier.com/locate/tca

Short communication

Solid–liquid interfacial energy for solid succinonitrile in equilibrium with succinonitrile dichlorobenzene eutectic liquid

Y. Ocak[a], S. Akbulut[a], U. Böyük[a], M. Erol[b], K. Keşlioğlu[a], N. Maraşlı[a,*]

[a] *Erciyes University, Faculty of Arts and Sciences, Department of Physics, 38039 Kayseri, Turkey*
[b] *Erciyes University Faculty of Arts and Sciences, Department of Physics, 66100 Yozgat, Turkey*

Received 6 February 2006; received in revised form 9 March 2006; accepted 10 March 2006
Available online 18 April 2006

Abstract

The equilibrated grain boundary groove shapes for solid succinonitrile (SCN) in equilibrium with the succinonitrile (SCN) dichlorobenzene (DCB) eutectic liquid were directly observed. From the observed grain boundary groove shapes, the Gibbs–Thomson coefficient and solid–liquid interfacial energy for solid SCN in equilibrium with the SCN DCB eutectic liquid have been determined to be $(5.43 \pm 0.27) \times 10^{-8}$ K m and $(7.95 \pm 0.80) \times 10^{-3}$ J m^{-2} with present numerical method and Gibbs–Thomson equation, respectively. The grain boundary energy of SCN rich phase of the SCN DCB eutectic system has been determined to be $(14.77 \pm 1.77) \times 10^{-3}$ J m^{-2} from the observed grain boundary groove shapes. Thermal conductivity of eutectic solid phase and eutectic liquid phase at the eutectic melting temperature have also been measured to be 0.269 and 0.231 W/K m, respectively.

Keywords: Crystal growth; Eutectic solidification; Interfacial energy; Grain boundary energy; Thermal conductivity

1. Introduction

The solid–liquid interfacial energy, σ_{SL}, is the reversible work required to create a unit area of the interface and plays a central role in determining the nucleation rate and growth morphology of crystals. The measurement of σ_{SL} in pure materials and alloys is difficult. One of the most common techniques to determine the solid–liquid interface energy is to use the equilibrated grain boundary groove shapes. In this technique, the solid–liquid interface is equilibrated with a grain boundary in a temperature gradient as shown in Fig. 1. The Gibbs–Thomson coefficient and solid–liquid interfacial energy are obtained using the equilibrium shape of the groove profile. This technique has been used to directly measure the solid–liquid interfacial energy for transparent materials [1–14] and for opaque materials [15–22].

Recently, the phase diagram of SCN DCB eutectic based system has been determined [23] and the thermo physical and chemical properties of SCN are well established. Thus, the goal of the present work is to determine the Gibbs–Thomson coefficient, solid–liquid interfacial energy and grain boundary energy for solid SCN in equilibrium with the SCN DCB eutectic liquid.

2. Experimental details

2.1. Sample production

The equilibrated solid SCN in equilibrium with the SCN DCB eutectic liquid have been directly observed by a temperature gradient stage. The details of the apparatus and experimental procedures are given in Refs. [9–11]. The specimen cell was made by sticking two glass cover slips (50 mm × 24 mm × 0.15 mm) with silicone elastomer glue. The slides were placed with their largest surface in the *x*–*y* plane and spaced a distance of about 80–100 μm apart in the *z* direction to minimize heat flow and curvature in the *z* direction and observe the equilibrated grain boundary groove shapes in *x*–*y* plane (2D). Organic materials usually react with this type glue. Before filling the cell with alloy, the cell was annealed at 523 K to prevent the reaction with glue.

In the present work, the alloy composition was chosen to be SCN–1 mol% DCB to observe the solid SCN in equilibrium with

---

* Corresponding author. Tel.: +90 352 4374901x33114; fax: +90 352 4374933.
E-mail address: marasli@erciyes.edu.tr (N. Maraşlı).

0040-6031/$ – see front matter © 2006 Elsevier B.V. All rights reserved.
doi:10.1016/j.tca.2006.03.014

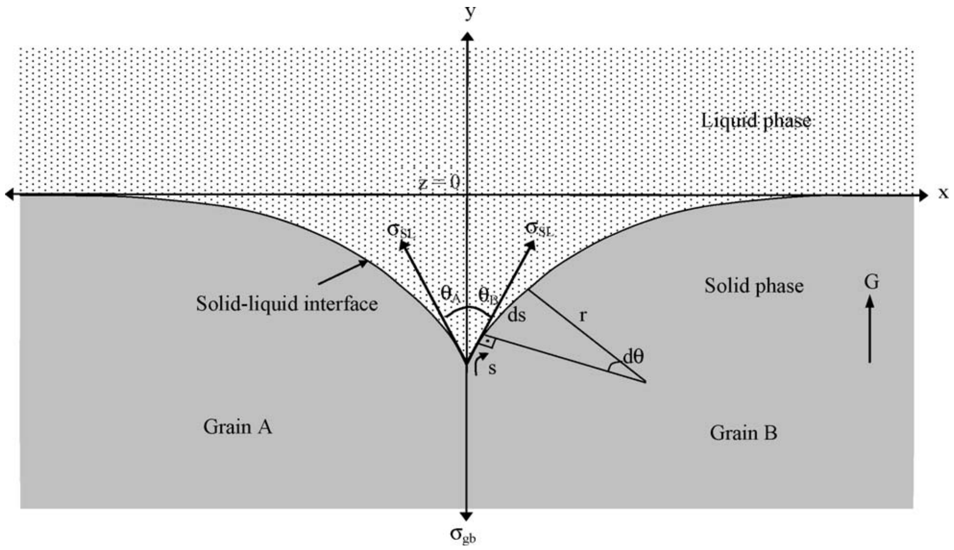

Fig. 1. Schematic illustration of an equilibrated grain boundary groove formed at a solid–liquid interface in a temperature gradient showing the *x*, *y* coordinates and *θ* angle.

the eutectic liquid (SCN–5.7 mol% DCB liquid). SCN–1 mol% DCB alloy was prepared from the >99% purity SCN and 99% purity DCB supplied by Sigma–Aldrich Chemical Company. No attempt was made to purify the compounds. Known masses of SCN and DCB were placed in a flask. The flask was then tightly sealed and heated in a hot water bath. Thus, an alloy was formed by the mixing of the components.

2.2. The temperature gradient measurement

After the specimen cell filled with organic alloy, the specimen was placed in temperature gradient stage. One side of the specimen was heated and the other side of the specimen was kept cool with a cooling system to get a constant temperature gradient on the specimen. The temperature of the heating system was controlled to an accuracy ±0.01 K with a Eurotherm 2604 type controller and the temperature of cooling system was kept constant (283 K) to an accuracy ±0.01 K with a PolyScience Digital 9102 Model Heating/Refrigerating circulating Baths. The temperatures in the specimen were measured using three insulated K-type thermocouples wires with 50 μm thick. One end of the thermocouple wires was spark welded. Thermocouples were placed at a distance about 1–2 mm from each other and perpendicular to the heat flow direction in the specimen.

A thin liquid layer (2 or 3 mm thick) was melted to get uniform eutectic liquid and the specimen was annealed in a constant temperature gradient. The annealing time was 2 days for SCN–1 mol% DCB alloy. When the solid–liquid interface reached equilibrium, the temperature differences between two thermocouples, ΔT were measured using a Hewlett-Packard 34401A model digital multimeter. The multimeter has a 1 μV resolution for direct voltage measurements. The positions of the thermocouples and the equilibrated grain boundary groove shapes were then photographed with a CCD digital camera placed on the top of Olympus BH2 light optical microscope. The distance between two thermocouples, ΔX was measured from the photographs of the thermocouple's positions using Adobe PhotoShop 7.0 version software.

The temperature gradient, $G = \Delta T/\Delta X$ for the equilibrated grain boundary groove shapes was determined using the values of ΔT and ΔX. The estimated error in the measurements of temperature gradient, G is about 5% [11].

The coordinates of equilibrated grain boundary groove shapes were measured with an optical microscope to an accuracy of ±10 μm. The uncertainty in the measurements of equilibrated grain boundary coordinates was 0.1%.

2.3. Thermal conductivity ratio of liquid phase to solid phase

The thermal conductivity ratio of the eutectic liquid phase (SCN–5.7 mol% DCB) to solid phase (SCN), $R = K_{\mathrm{L(eutectic\ liquid)}}/K_{\mathrm{S(solid\ SCN)}}$ must be known or measured to evaluate the Gibbs–Thomson coefficients with the present numerical method. The radial heat flow method is an ideal technique for measuring the conductivities in the solid. The thermal conductivity of the eutectic solid phase, $K_{\mathrm{S(eutectic\ solid)}}$ is needed to evaluate the thermal conductivity of the eutectic liquid phase, $K_{\mathrm{L(eutectic\ liquid)}}$. In the radial heat flow method, a cylindrical sample was heated by using a single heating wire along the axis at the centre of the sample and the sample was kept in a very stable temperature gradient for a period to achieve the steady-state condition. At the steady-state condition, the temperature gradients in the cylindrical specimen is given by Fourier's law

$$\frac{\mathrm{d}T}{\mathrm{d}r} = -\frac{Q}{AK_{\mathrm{S}}} \tag{1}$$

where Q is the total input power from the centre of the specimen, A is the surface area of the specimen which is normal to the heat flow direction and K_{S} is the thermal conductivity of solid phase.

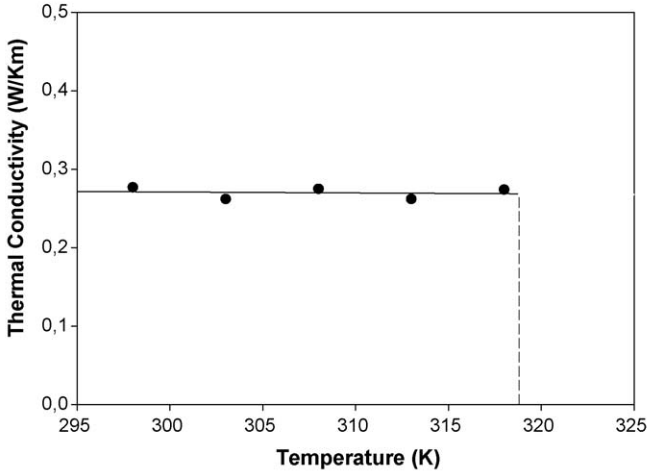

Fig. 2. Thermal conductivities of solid SCN–5.7 mol%DCB phase vs. temperature.

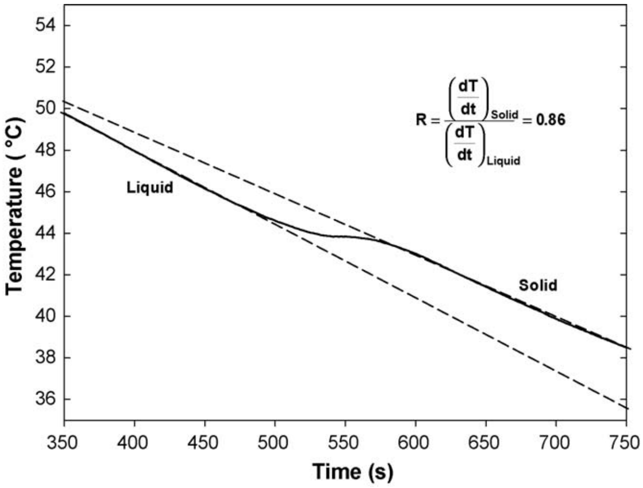

Fig. 3. Temperatures vs. time for SCN–5.7 mol%DCB alloy.

Integration of the Eq. (1) gives

$$K_S = \frac{1}{2\pi\ell}\ln\left(\frac{r_2}{r_1}\right)\frac{Q}{T_1 - T_2} \tag{2}$$

$$K_S = a_0\frac{Q}{T_1 - T_2} \tag{3}$$

where $a_0 = \ln(r_2/r_1)/2\pi\ell$ is an experimental constant, r_1 and $r_2 (r_2 > r_1)$ are fixed distances from the centre of the specimen, ℓ is the length of the heating wire which is constant and T_1 and T_2 are the temperatures at the fixed positions, r_1 and r_2 from the centre of specimen. Eq. (3) could be used to give the conductivity of solid phase by measuring the difference in the temperatures between the fixed two points for a given power level.

The thermal conductivity of eutectic solid phase, $K_{S(\text{eutectic solid})}$ was measured with a radial heat flow apparatus. The details of the radial heat flow apparatus and technique are given in Refs. [15,19,24]. The sample was heated using the central heating wire in steps of 5 up to 2 K bellow the eutectic melting temperature. The samples were kept at steady-state for at least 2 h. At steady-state the total input power and the temperatures were measured. When all desired power and temperature measurements had been completed the sample was left to cool down to room temperature. The process was repeated at least three times to give average values. The thermal conductivities of eutectic solid phase (SCN–5.7 mol% DCB) versus temperature is shown in Fig. 2. The value of thermal conductivity of $K_{S(\text{eutectic solid})}$ at the eutectic melting temperature were obtained to be 0.269 W/(K m) by extrapolating to the eutectic temperature.

The thermal conductivity ratio of the eutectic liquid phase (SCN–5.7 mol% DCB) to eutectic solid phase (SCN–5.7 mol% DCB), $R = K_{L(\text{eutectic liquid})}/K_{S(\text{eutectic solid})}$ were measured in a directional growth apparatus. The time-temperature trace enables the conductivity ratio of the liquid phase to solid phase to be calculated [15–17]. The thermal conductivity ratio of eutectic liquid phase to eutectic solid phase $R = K_{L(\text{eutectic liquid})}/K_{S(\text{eutectic solid})}$ was found to be 0.86 from the time–temperature trace which is given in Fig. 3. Thus, the thermal conductivity of eutectic liquid phase, $K_{L(\text{eutectic liquid})}$ is obtained to be 0.2310 W/(K m). The measured values of thermal conductivities for SCN DCB eutectic system are given in Table 1. The value of $K_{S(\text{solid SCN})}$ is 0.2244 W/(K m) [24]. The value of $R = K_{L(\text{eutectic liquid})}/K_{S(\text{solid SCN})}$ was found to be 1.03 and it is also given in Table 1.

3. Results and discussions

3.1. The Gibbs–Thomson coefficient

If the thermal conductivity ratio of the equilibrated liquid phase to solid phase, $R = K_L/K_S$, the coordinates of the grain boundary groove shapes and the temperature gradient in the solid phase, G are known, then the Gibbs–Thomson coefficient can be obtained using the numerical method described in detail in

Table 1
The thermal conductivity of solid and liquid phases and their ratios at their eutectic temperatures for pure SCN and SCN DCB binary eutectic system

System	Phases	Temperature (K)	K W/(K m)	$R = K_L/K_S$
SCN	Solid SCN	331.23	0.2244 [25]	0.99
	Liquid SCN		0.2219 [25]	
Eutectic SCN DCB	Solid (SCN–5.7 mol DCB)	319.15	0.2690	0.86
	Liquid (SCN–5.7 mol DCB)		0.2310	
SCN DCB	Solid SCN	319.15	0.2244 [25]	1.03
	Liquid (SCN–5.7 mol DCB)		0.2310	

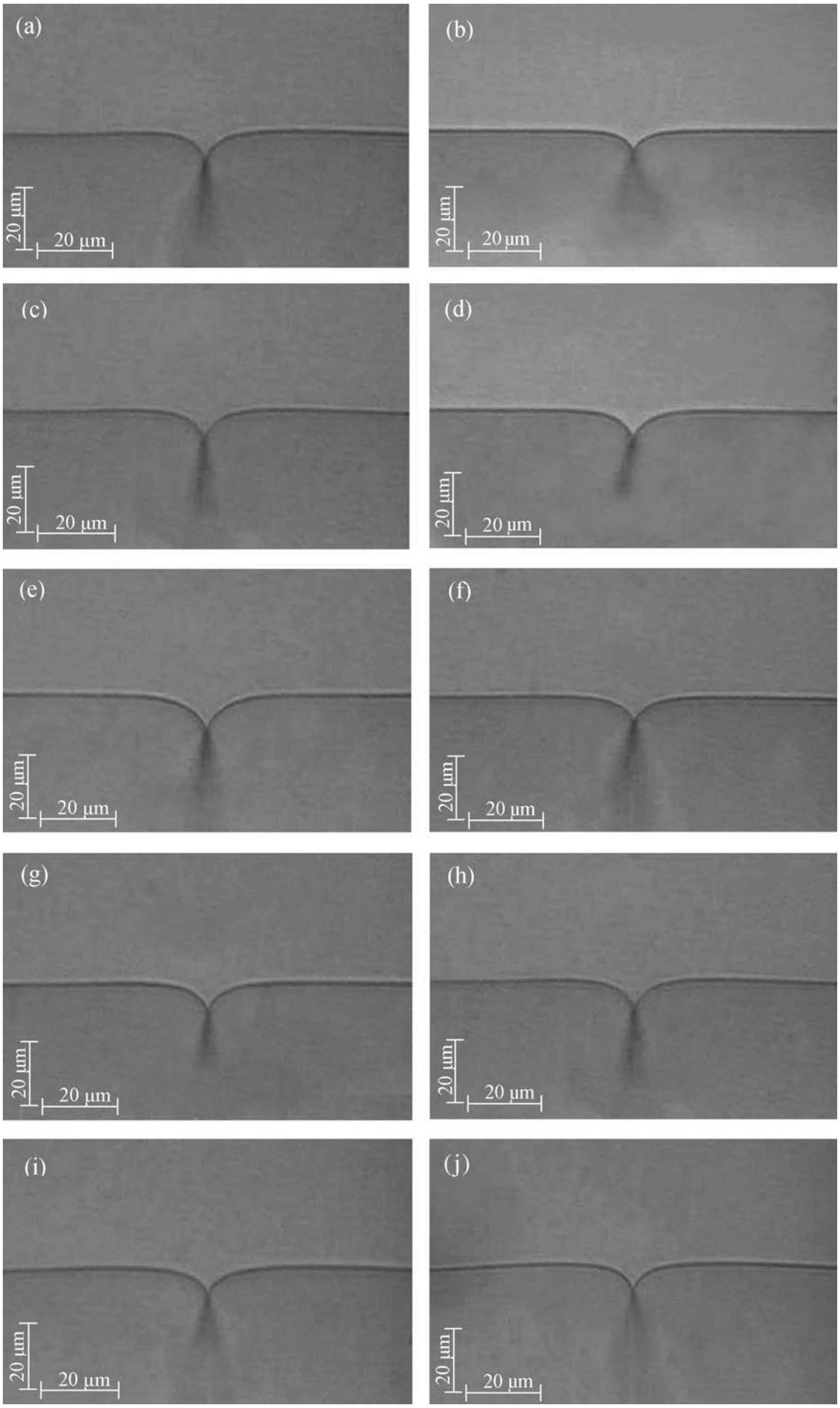

Fig. 4. Typical grain boundary groove shapes for solid SCN in equilibrium with the SCN DCB eutectic liquid.

Ref. [15]. As mentioned above, the experimental error in the determination of Gibbs–Thomson coefficient was about 5%.

The Gibbs–Thomson coefficients for solid SCN in equilibrium with the SCN DCB eutectic liquid were determined by the numerical method using 10 observed grain boundary groove shapes and the results are given in Table 2. Typical grain boundary groove shapes for solid SCN in equilibrium with the SCN DCB eutectic liquid examined in present work are shown in Fig. 4.

The average value of Γ with experimental error from Table 2 is $(5.43 \pm 0.27) \times 10^{-8}$ K m for solid SCN in equilibrium with the SCN DCB eutectic liquid.

Table 2
Gibbs–Thomson coefficients for solid SCN in equilibrium with SCN DCB eutectic liquid

Groove no.	$G_S \times 10^2$ (K/m)	Gibbs–Thomson coefficient Γ (K m)	
		$\Gamma_{LHS} \times 10^{-8}$	$\Gamma_{RHS} \times 10^{-8}$
a	76.51	5.55	5.33
b	75.78	5.40	5.46
c	77.37	5.36	5.42
d	79.95	5.42	5.40
e	76.63	5.40	5.55
f	79.95	5.44	5.51
g	76.63	5.42	5.32
h	75.78	5.36	5.53
i	75.21	5.30	5.40
j	70.42	5.60	5.40

$\bar{\Gamma} = (5.43 \pm 0.27) \times 10^{-8}$ K m for solid SCN in equilibrium with SCN DCB eutectic liquid.

Table 3
The effective entropy change per unit volume, ΔS^* for SCN DCB eutectic system

System	SCN DCB
Solid phase (C_S)	SCN
Liquid phase (C_L) (eutectic point)	SCN–5.71 mol% DCB
T_M	319.15 (K)
$V_S \times 10^{-6}$ (SCN)	76.5 (m^3/mol) [26]
$\Delta S^* \times 10^5$	11.2 ($J\,K^{-1}\,mol^{-1}$) [23]

3.2. The effective entropy change

To calculate the solid–liquid interface energy, it is also necessary to know the effective entropy change per unit volume. The effective entropy change per unite volume is given by:

$$\Delta S^* = \frac{\Delta H}{T_M}\frac{1}{V_S} \qquad (4)$$

where ΔH is the enthalpy of primary phase in the binary eutectic system, T_M is the melting temperature and V_S is the molar volume of primary phase. The values of T_M, V_S and ΔS^* are given in Table 3.

3.3. The solid–liquid interface energy

The solid–liquid interface energy, σ_{SL} is obtained from the thermodynamic definition of the Gibbs–Thomson coefficient [15], which is expressed as:

$$\Gamma = \frac{\sigma_{SL}}{\Delta S^*} \qquad (5)$$

where ΔS^* is the entropy change of fusion per unit volume.

If the values of the Gibbs–Thomson coefficient and the effective entropy change per unit volume are measured or known, the solid–liquid interface energy can be obtained from Eq. (5). The experimental error in the determined solid–liquid interface energy is the sum of experimental errors of Gibbs–Thomson coefficient and effective entropy change per unit volume. Experimental error for the solid–liquid interface energy measurements with the present method is about 10% [11]. The value of the solid–liquid interfacial energy for solid SCN in equilibrium with the SCN DCB eutectic liquid was found to be $(7.95 \pm 0.80) \times 10^{-3}\,J\,m^{-2}$.

3.4. The grain boundary energy

The grain boundary energy can be expressed by:

$$\sigma_{gb} = 2\sigma_{SL}\cos\theta \qquad (6)$$

where $\theta = \theta_A + \theta_B/2$ is the angle that the solid–liquid interfaces make with the y axis [11,27]. The angles, θ_A and θ_B were obtained from the cusp coordinates, x, y using a Taylor expansion for parts at the base of the groove. The grain boundary energy was then calculated from Eq. (6) using the solid–liquid interface energy and the values of θ. The estimated error in determination of angles was found to be 2% from standard deviation. Thus, the total experimental error in the resulting grain boundary energy is about 12%. The value of σ_{gb} for solid SCN was found to be $(14.77 \pm 1.77) \times 10^{-3}\,J\,m^{-2}$.

A comparison of the experimental results obtained in present work with previous measurements of the Gibbs–Thomson coefficient, solid–liquid interface energy and grain boundary energy for pure SCN and SCN bases binary eutectic alloys is given in Table 4. As can be seen from Table 4, our results are in good agreement with the values found in literature.

Table 4
A comparison with the previous measurements of the Gibbs–Thomson coefficient, solid–liquid interface energy and grain boundary energy for the SCN DCB eutectic system obtained in the present work

System	Solid phase	Liquid phase	$\Gamma \times 10^{-8}$ (K m)	$\sigma_{SL} \times 10^{-3}$ ($J\,m^{-2}$)	$\sigma_{gb} \times 10^{-3}$ ($J\,m^{-2}$)
Pure SCN	SCN	SCN	6.17 5.54 [11]	8.94 ± 0.5 [4] 8.02 [11]	15.95 [11]
SCN	SCN	SCN	5.43 ± 0.27 [11]	7.86 ± 0.79 [11]	15.03 ± 1.95 [11]
SCN–CTB	SCN	SCN–4 mol% CTB	5.56 ± 0.28 [11]	8.80 ± 0.88 [11]	16.51 ± 2.15 [11]
PY–SCN	SCN	SCN–25.6 mol% PY	5.21 ± 0.26 [13]	9.58 ± 0.96 [13]	18.30 ± 2.38 [13]
SCN–DC	SCN–0.16 mol% DC	SCN–13.9 mol% DC	5.39 ± 0.27 [14]	7.88 ± 0.79 [14]	14.95 ± 1.79 [14]
SCN DCB	SCN	SCN–5.71 mol% DCB	5.43 ± 0.27 [present]	7.95 ± 0.80 [present]	14.77 ± 1.77 [present]

4. Conclusions

The equilibrated grain boundary groove shapes for solid SCN in equilibrium with the SCN DCB eutectic liquid were directly observed. From the observed grain boundary groove shapes, the Gibbs–Thomson coefficient, solid–liquid interface energy and the grain boundary energy for solid SCN in equilibrium with the SCN DCB eutectic liquid have been determined. Thermal conductivities of eutectic solid phase and eutectic liquid phase at the eutectic melting temperature have also been measured.

Acknowledgements

This project was supported by the Erciyes University Research Foundation under Contract No. FBT-06-38. Authors would like to thank Erciyes University Research Foundation for their financial supports.

References

[1] D.R.H. Jones, G.A. Chadwick, Philos. Mag. 22 (1970) 291.
[2] D.R.H. Jones, G.A. Chadwick, J. Cryst. Growth 11 (1971) 260.
[3] D.R.H. Jones, Philos. Mag. 27 (1978) 569.
[4] R.J. Schaefer, M.E. Glicksman, J.D. Ayers, Philos. Mag. 32 (1975) 725.
[5] S.C. Hardy, Philos. Mag. 35 (1977) 471.
[6] G.E. Nash, M.E. Glicksman, Philos. Mag. 24 (1971) 577.
[7] G.F. Bolling, W.A. Tiller, J. Appl. Phys. 31 (1960) 1345.
[8] N.B. Singh, M.E. Glicksman, J. Cryst. Growth 98 (1989) 573.
[9] B. Bayender, N. Maraşlı, E. Çadırlı, H. Şişman, M. Gündüz, J. Cryst. Growth 194 (1998) 119.
[10] B. Bayender, N. Maraşlı, E. Çadırlı, M. Gündüz, Mater. Sci. Eng. A 270 (1999) 343.
[11] N. Maraşlı, K. Keşlioğlu, B. Arslan, J. Cryst. Growth 247 (2003) 613.
[12] I. Stalder, J.H. Bilgram, J. Chem. Phys. 118 (2003) 798.
[13] U. Böyük, K. Keşlioğlu, M. Erol, N. Maraşlı, Mater. Lett. 59 (2005) 2953.
[14] K. Keşlioğlu, U. Böyük, M. Erol, N. Maraşlı, J. Mater. Sci. (2006), in press.
[15] M. Gündüz, J.D. Hunt, Acta Metall. 33 (1985) 1651.
[16] M. Gündüz, J.D. Hunt, Acta Metall. 37 (1989) 1839.
[17] N. Maraşlı, J.D. Hunt, Acta Mater. 44 (1996) 1085.
[18] K. Keşlioğlu, N. Maraşlı, Mater. Sci. Eng. A 369 (2004) 294.
[19] K. Keşlioğlu, N. Maraşlı, Metall. Mater. Trans. A 35A (2004) 3665.
[20] K. Keşlioğlu, M. Gündüz, H. Kaya, E. Çadırlı, Mater. Lett. 58 (2004) 3067.
[21] M. Erol, N. Maraşlı, K. Keşlioğlu, M. Gündüz, Scripta Mater. 51 (2004) 131.
[22] K. Keşlioğlu, M. Erol, N. Maraşlı, M. Gündüz, J. Alloys Compd. 385 (2004) 207.
[23] R.N. Rai, U.S. Rai, Thermochim. Acta 363 (2000) 23–28.
[24] M. Erol, K. Keşlioğlu, R. Şahingöz, N. Maraşlı, Met. Mater. Int. 11 (2005) 421–428.
[25] B. Kauerauf, G. Zimmermann, L. Murmann, S. Rex, J. Cryst. Growth 193 (1998) 701–711.
[26] P. Derollez, J. Lefebvre, M. Descamps, W. Press, H. Fontaine, Conden. Matter 2 (1990) 6893.
[27] D.P. Woodruff, The Solid–Liquid Interface, Cambridge University Press, Cambridge, 1973.